

Properties of Ce-based bulk metallic glass-forming alloys

Bo Zhang, R. J. Wang, D. Q. Zhao, M. X. Pan, and W. H. Wang*

Institute of Physics, Chinese Academy of Sciences, Beijing 100080, China

(Received 24 April 2004; revised manuscript received 18 June 2004; published 17 December 2004)

We find that a family of CeAlNiCu alloy system can be readily cast into bulk glassy rods with up to 3 mm diameter. The Ce-based bulk metallic glasses (BMG's) exhibit a wide supercooled region up to 78 K, very low glass transition temperature ($T_g=359$ K), and Debye temperature ($\theta_D=144$ K). The glass formation, crystallization, glass transition, liquid behavior, and elastic and acoustic properties of the CeAlNiCu alloys are investigated. Ultrasonic measurements demonstrate that the Ce-based BMG's are the softest in elastic moduli in known BMG's due to their very low glass transition temperature. The fragility parameter (m) is determined to be 21, indicating the strong liquid behavior of the alloy concerning the temperature dependence of viscosity. A remarkable large softening of long-wavelength acoustic phonons in the BMG relative to its crystalline state is observed, and the phonon softening is attributed to its intrinsic microstructural features and strong liquid behavior.

DOI: 10.1103/PhysRevB.70.224208

PACS number(s): 61.43.Fs, 61.25.Mv, 62.65.+k, 64.70.Dv

I. INTRODUCTION

In the past decades, a series of metallic alloys formed at a critical cooling rate of less than 100 K/s in the bulk via conventional casting have been discovered.^{1,2} The family of metallic glasses with unique mechanical properties and the ease of moldinglike polymers has promise for applications such as new structural materials.^{1,2} In fact, the bulk metallic glasses (BMG's) based on conventional transition metals such as Zr, Fe, Ni, Co, Ti, Mg, and Cu are being mainly developed for potential applications as engineering materials.^{1,2} The rare-earth (RE) based BMG's, however, could have potentials for application as functional materials.²⁻⁵ Cerium is a typical and most abundant RE metal on earth.⁶ One of the intrinsic features of Ce is its variable electronic structure and dual valency states, because of which only small amount of energy is required to change the relative occupancy of the electronic levels. For example, when Ce is subjected to high pressure or low temperatures a volume change of approximately 10% results.⁶ Therefore the structural and physical properties of the Ce-based BMG's could have characteristics which are different from those of other known BMG's.

The efforts in the past to understand the puzzle of the glass transition and relaxation had mostly been connected with chainlike or network forming substances.^{7,8} Amorphous alloys are the paradigm of a dense random packing structure, and they are comparable to a hard-sphere system, rather easily describable in contrast to inorganic, nonmetallic glass formers and organic polymers.^{7,8} The BMG's with obvious glass transition and stable supercooled liquid state are an ideal system for investigating supercooled liquid state with a large experimentally accessible time and temperature window. As an effective way to evaluate the relaxation dynamics of supercooled liquids, the concept of fragility was introduced by Angell.^{7,8} In fact, the fragility parameter, m is not only a general dynamic parameter, but also a sensitive parameter to the structure of the glass-forming liquid. However, what structural information that the fragility parameter suggests and the relation between the structure and the fra-

gility parameter of the studied glass-forming system have less been studied in BMG's.

In this work, a family of Ce-based BMG's with excellent glass-forming ability (GFA) is developed. The glass formation, crystallization, glass transition, liquid behavior, and elastic and acoustic properties of the alloys are investigated. The key temperatures (T_g , Kauzmann temperature T_K , Vogel-Fulcher temperature T_0) and fragility parameter (m), which are often used to characterize vitrification and properties of a supercooled liquid or a glass, are determined for the typical Ce-based BMG. The BMG is found to show strong liquid behavior concerning its temperature dependence of viscosity. The elastic constants, measured by the ultrasonic technique, are of the lowest values in known BMG's and are comparable with those of polymers and other nonmetallic glasses, showing that the Ce-based BMG's are the softest in elastic moduli among metallic glasses. Moreover, a remarkable softening in elastic behavior of phonons of the BMG relative to its crystallized state has been observed which are mainly attributed to the intrinsic glassy structure and strong liquid behavior of the Ce-based alloys.

II. EXPERIMENTAL

The Ce-Ni-Al-Cu alloys with nominal compositions listed in Table I were prepared by arc melting pure Cu, Ni, Al, and Nb with industrial pure Ce in a Ti-gettered argon atmosphere. The purity of Ce was only about 99.5 wt.%, which was much lower than that of other base elements of BMG's. The alloy ingots were remelted and suck cast into a Cu mold to get cylindrical rods in different diameters. The structure of the as-cast alloys was ascertained by x-ray diffraction (XRD) using a MAC M03 XHF diffractometer with Cu $K\alpha$ radiation. The differential scanning calorimeter (DSC) measurements were carried out under a purified argon atmosphere in a Perkin Elmer DSC7 at the heating rate, ϕ , ranging from 2 to 200 K/min. Calorimeter was calibrated for temperature and energy at various heating rates with high purity indium and zinc. First, an empty Al pan was performed to establish

TABLE I. The values of the T_g , T_x , T_m , T_l , γ , T_{RG} , and the critical diameters of fully amorphous rod of the Ce-based BMG's. The data for other typical BMG's adopted from Refs. 12–14, are also listed for comparison.

Alloy system	Critical diameter (mm)	T_g (K)	T_x (K)	T_m (K)	T_l (K)	ΔT (K)	T_{RG}	γ
Ce ₆₀ Al ₁₀ Ni ₁₀ Cu ₂₀	1	373	426	649	677	53	0.57	0.406
Ce ₇₀ Al ₁₀ Ni ₁₀ Cu ₁₀	3	359	377	639	714	18	0.56	0.351
Ce ₆₅ Al _{12.5} Ni _{12.5} Cu ₁₀	3	371	402	644	709	31	0.58	0.372
Ce ₆₀ Al ₁₅ Ni ₁₅ Cu ₁₀	3	390	468	644	685	78	0.61	0.435
Ce ₆₅ Al ₁₀ Ni ₁₀ Cu ₁₀ Nb ₅	5	359	384	637	702	25	0.56	0.362
Ce ₅₇ Al ₁₀ Ni _{12.5} Cu _{15.5} Nb ₅	2	369	415	638	677	46	0.58	0.397
Zr ₆₅ Al _{7.5} Cu _{17.5} Ni ₁₀		656	735	1108	1168	79	0.59	0.403
Zr _{41.2} Ti _{13.8} Cu _{12.5} Ni ₁₀ Be _{22.5}		623	672	932	996	49	0.67	0.415
Pd ₄₀ Ni ₁₀ Cu ₃₀ P ₂₀		575	670	804	840	95	0.72	0.473

a baseline, and then the same Al pan including the sample was carried out again at the identical thermal condition. The values of the T_g , and the onset temperature for crystallization peak (T_x) were determined from the DSC traces with the accuracy of ± 1 K. The annealing experiments for the Ce-based BMG's were performed in vacuum chamber (better than 10^{-3} Pa) at a temperature 100 K above crystallization temperature for 1 h.

The acoustic velocities of the Ce-based alloys were measured using a pulse echo overlap method by a MATEC 6600 model ultrasonic system with a measuring sensitivity of 0.5 ns.⁹ The sample rod was cut to a length of about 6 mm, and its ends were carefully polished flat and parallel. The excitation and detection of the ultrasonic pulses were provided by X- or Y-cut (for longitudinal and transverse waves, respectively) quartz transducers. The density ρ was determined by the Archimedeian technique and the accuracy lies within 0.1%. Elastic constants (e.g., the Young's modulus E , the shear modulus G , and the bulk modulus K) and the Debye temperature θ_D were derived from the acoustic velocities and the density.⁹

III. RESULTS AND DISCUSSIONS

A. Formation of Ce-based BMG's

Figure 1(a) shows the XRD pattern of a typical as-cast Ce₆₀Al₁₀Ni₁₀Cu₂₀ BMG in cylinder-shaped rod with diameter of 1 mm. The XRD curve shows the broad diffraction maximum characteristic of amorphous structure and without any clearly visible diffraction peaks corresponding to crystalline phases. With the composition modification, the BMG rods such as Ce₇₀Al₁₀Ni₁₀Cu₁₀ extend to 3 mm in diameter. If more components such as Nb are introduced, the BMG rod can be further extended to 5 mm. Figure 1(b) is the DSC trace of the Ce₆₀Al₁₀Ni₁₀Cu₂₀ BMG at a heating rate of 10 K/min. The crystallization process is single exothermic reaction. The remarkable features of the trace are an obvious endothermic characteristic before crystallization indicating an obvious glass transition onset at 373 K and a large supercooled liquid region ΔT ($\Delta T = T_x - T_g$) of 53 K. From the endothermic signal of the melting [Fig. 1(c)], one can see

that the composition of the alloy is not near eutectic composition point. The T_x , melting temperature T_m , and liquidus temperatures T_l are determined to be 427, 649, and 677 K, respectively. The reduced glass transition temperature T_{RG} ($T_{RG} = T_g/T_m$),¹⁰ and γ value [$\gamma = T_x/(T_g + T_l)$]¹¹, which are critical parameters in determining the GFA of an alloy, are 0.57 and 0.406, respectively. The distinct glass transition and sharp crystallization and large values of T_{RG} and γ further confirm the glassy structure and highly GFA of the Ce-based alloy. For comparison, the thermal parameters and the parameters in determining the GFA of the Ce-based BMG and other typical BMG's (Ref. 4 and 12–14) are listed in Table I. Compared with the other typical BMG's, such as Zr_{41.2}Ti_{13.8}Cu_{12.5}Ni₁₀Be_{22.5} and PdCuNiP alloys, the Ce-based BMG's have moderate high GFA but much lower T_g and T_m . According to the glass formation criteria,^{1,2} the sufficient atomic radius differences among Ce (atomic radius, $r = 1.82$ Å), Al ($r = 1.43$ Å), Ni ($r = 1.25$ Å), and Cu ($r = 1.28$ Å),¹⁵ the larger negative heat of mixing between Ce and other components [e.g., for Ce-Ni, the heat of mixing is -43 KJ/mol (Ref. 16)], and multi-component result in the excellent GFA.

The CeNiAlCu alloys can be cast into BMG in a large composition range. Figure 2 shows the DSC results of the

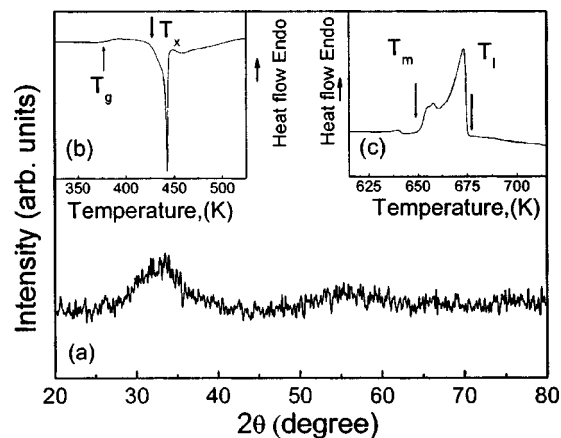


FIG. 1. (a) XRD patterns of the as-cast Ce₆₀Al₁₀Ni₁₀Cu₂₀ alloy. (b) DSC trace of crystallization and glass transition processes. (c) Melting process of the Ce₆₀Al₁₀Ni₁₀Cu₂₀ alloy.

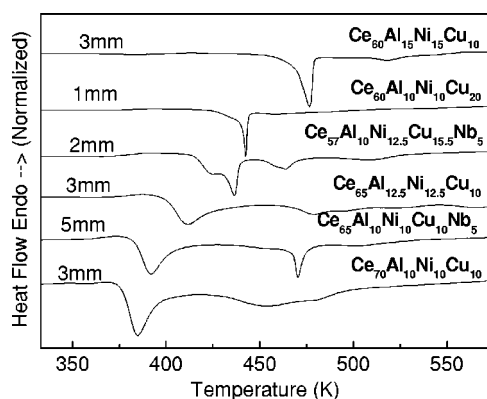


FIG. 2. DSC traces of the Ce-based BMG's with different compositions and critical diameters.

BMG's with different compositions and critical diameters. The crystallization process of these BMG's is sensitive to the composition as shown in Fig. 2. With composition modification, the T_g of the $\text{Ce}_{70}\text{Al}_{10}\text{Ni}_{10}\text{Cu}_{10}$ BMG can be as low as 359 K, which is the lowest value in known BMG's. The $\text{Ce}_{60}\text{Al}_{15}\text{Ni}_{15}\text{Cu}_{10}$ alloy has the highest $T_g=390$ K, the largest $\Delta T_x=78$ K, the largest T_{RG} , (0.61) and γ (0.435) among the Ce-based BMG's. The addition of Nb can increase the critical diameter of the BMG, and further decrease T_g and increase ΔT of the alloys. From Table I, the T_{RG} , γ , and the GFA (represented by critical diameter) do not show the same trend as other BMG's do.^{11,12}

E , G , K , and θ_D of the representative $\text{Ce}_{70}\text{Al}_{10}\text{Ni}_{10}\text{Cu}_{10}$ BMG, obtained from acoustic measurements, are 30.3, 11.5, and 27.0 GPa and 144 K, respectively. To our best knowledge, these are the lowest elastic constants among metallic glasses so far. The elastic values are comparable to those of amorphous carbon and oxides fused quartz, and close to those of polymers listed in Table II, indicating that the BMG's exhibit elastic properties similar to those of nonmetallic glasses, and have much softer elastic constants than those of other BMG's.^{17,18} The softer behavior in elastic constants compared to other BMG's may be due to the low glass transition temperature of the alloys, because the elastic moduli have been found to have correlation with the glass transition temperature in various BMG's.¹⁷

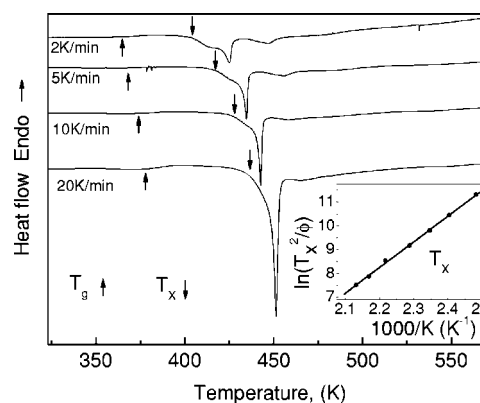


FIG. 3. DSC traces of $\text{Ce}_{60}\text{Al}_{10}\text{Ni}_{10}\text{Cu}_{20}$ BMG at different heating rates from 2 to 20 K/min. The inset shows the Kissinger plot of the T_x .

B. Crystallization of the Ce-based BMG's

Crystallization studies of the metallic glasses are of importance in understanding the mechanism of phase transformations far from equilibrium and in evaluating the GFA of an alloy. Figure 3 shows the DSC curves of the $\text{Ce}_{60}\text{Al}_{10}\text{Ni}_{10}\text{Cu}_{20}$ BMG at different heating rates. The crystallization peak shifts to higher temperature with increasing heating rate as shown in Fig. 3, indicating the obvious kinetic behavior of crystallization. Figure 4 shows the dependence of the T_g , T_x , and ΔT_x upon ϕ at different heating rates from 2 to 200 K/min. The T_g , T_x , and ΔT_x increase faster at low heating rates and show similar tendency upon ϕ . The crystallization kinetics of the BMG is evaluated using Kissinger's equation¹⁹

$$\ln \frac{T_x^2}{\phi} = \frac{E_a}{T} + \ln \frac{E_a}{k_B K_0}, \quad (1)$$

where T is the crystallization characteristic temperature, k_B is Boltzman constant, K_0 is the frequency factor, and E_a is the apparent activation energy. The Kissinger plot of the T_x is shown in the inset of Fig. 3. The values of E_a and K_0 of the crystallization obtained from the Kissinger method are 1.33 eV and $1.87 \times 10^{13} \text{ s}^{-1}$, respectively. The activation energy can be interpreted as the additional energy that an atom must acquire in order to be a part of the activated cluster.^{19,20}

TABLE II. The acoustic data and elastic constants (e.g., E , G , K , and σ) and θ_D for the $\text{Ce}_{70}\text{Al}_{10}\text{Ni}_{10}\text{Cu}_{10}$ BMG, amorphous carbon, nonmetallic glasses, and $\text{Zr}_{41}\text{Ti}_{14}\text{Cu}_{12.5}\text{Ni}_{10}\text{Be}_{22.5}$ BMG. The data for other glasses are adopted from Refs. 16 and 17.

Glasses	ρ (g/cm ³)	V_l (km/s)	V_s (km/s)	E (GPa)	G (GPa)	K (GPa)	σ	θ_D (K)
$\text{Ce}_{70}\text{Al}_{10}\text{Ni}_{10}\text{Cu}_{10}$	6.670	2.521	1.315	30.3	11.5	27.0	0.313	144
Amorphous carbon	1.56	3.88	2.407	21.4	9.01	11.4	0.187	338
Nylon				4.0	1.43	6.54	0.40	
Polypropylene				4.13	1.54	4.37	0.34	
Polyethylene				2.55	0.91	4.54	0.41	
Fused quartz	2.201	5.96	3.75	72.7	31.0	36.9	0.17	496
$\text{Zr}_{41}\text{Ti}_{14}\text{Cu}_{12.5}\text{Ni}_{10}\text{Be}_{22.5}$	6.125	5.174	2.472	101.2	37.4	114.1	0.352	327

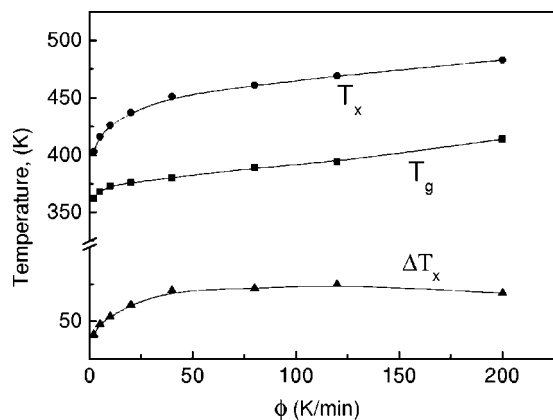


FIG. 4. The dependence of T_g , T_x , and ΔT_x of the $\text{Ce}_{60}\text{Al}_{10}\text{Ni}_{10}\text{Cu}_{20}$ BMG on the heating rate ϕ .

Compared with other BMG's,^{21–27} the Ce-based BMG shows fairly smaller value of E_a . Figure 5 shows a rough linear relation between E_a and T_x of a variety of typical BMG's, which presents a general trend that the BMG's with higher T_x have larger E_a . Crystallization takes place when the atoms have enough additional energy to become a part of the critical nuclei, and the conventional crystallization is induced by thermal activation. Therefore, the higher E_a needs high thermally activated temperature. The small E_a should be an intrinsic feature of the Ce-based BMG's which have much lower glass transition and crystallization temperatures.

C. Glass transition and fragility of the Ce-based alloy

The unique Ce-based BMG's should have intrinsic features in the supercooled liquid state. The large supercooled liquid region of the BMG offers great conveniences for investigation of the nature of the supercooled liquid in terms of the Angell's fragility concept.⁸ Figure 6 presents the dependence of T_g and T_x on $\ln \phi$ of the $\text{Ce}_{60}\text{Al}_{10}\text{Ni}_{10}\text{Cu}_{20}$ BMG from 2 to 200 K/min. Similar to crystallization, the glass transition of the BMG also exhibits obvious kinetic behavior, and the change of T_g upon ϕ follows the Lasocka's relationship²⁸ $T_g = 358.2 + 6.02 \ln \phi$ below the heating rate of 40 K/min, while T_x shows the linear relation with $\ln \phi$ as

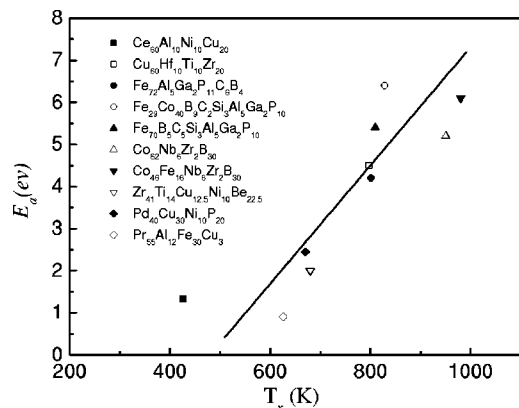


FIG. 5. The rough linear relation between E_a and T_x of the Ce-, Zr-, Pd-, Fe- Cu-, Co-, and Pr-based BMG's.

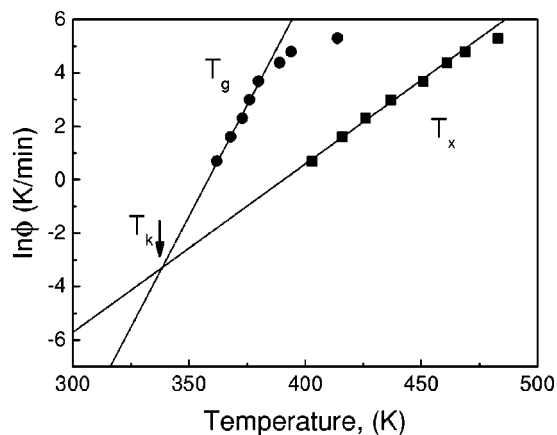


FIG. 6. The Lasocka's relationship of T_g , T_x , and ϕ of the $\text{Ce}_{60}\text{Al}_{10}\text{Ni}_{10}\text{Cu}_{20}$ BMG in the heating rate range of 2 to 200 K/min.

$T_x = 390.7 + 15.90 \ln \phi$ almost ranging from 2 to 200 K/min. This result suggests the different kinetic behaviors between the glass transition and crystallization. When extrapolating the dependence of T_g and T_x down to lower heating rate, the two curves intersect at 338 K shown in Fig. 6, which corresponds to a cooling rate of about 0.035 K/min and equals the Kauzmann temperature T_K within experimental error.²⁹ The difference between T_g (at 2 K/min) and T_K is 31 K, and much smaller than that of other BMG's.³⁰

For the BMG's, the linear fitting using the Lasocka's relation is not so convincing in describing their behavior at larger heating rates as shown in Fig. 6.^{31,32} When ϕ is extended to above 40 K/min, the linear relationship has a distinct divergence. Therefore, we try to fit the relationship of T_g and $\ln \phi$ with Vogel-Fulcher equation³²

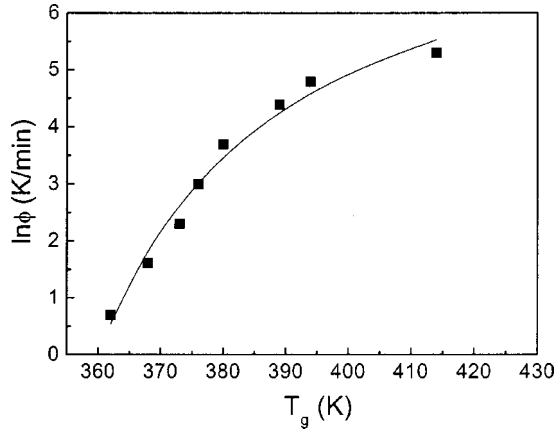
$$\ln \phi = \ln B - \frac{DT_0}{T_g - T_0}, \quad (2)$$

where B is a parameter representing the time scale in the glass-forming system,³² D is the strength parameter in the VFT equation, which controls how closely the liquid system obeys the Arrhenius law, and T_0 is the asymptotic value of T_g usually approximated as the onset of the glass transition within the limit of infinitely slow cooling and heating rate. The best fit is shown in Fig. 7 and the fitting parameters $\ln B$, D , and T_0 are 8.55, 0.76 and 331 K, respectively. The value of T_0 (=331 K) is very close to T_K (=338 K), implying that the metastable equilibrium supercooled liquid can exist close to T_K .

The fragility concept provides a measure of the sensitivity of the structure of a liquid to temperature changes,^{7,8} and can be used to classify glass-forming liquid into three general categories: strong, intermediate and fragile. The fragility can be quantified by the fragility parameter m defined as³³

$$m = \left. \frac{d \log \langle \tau \rangle}{d \langle T_g/T \rangle} \right|_{T=T_g}, \quad (3)$$

where $\langle \tau \rangle$ is the average relaxation time, and T the temperature. From the VFT fit the m at a particular T_g can be calculated from³⁴


 FIG. 7. VFT relationship between T_g and ϕ .

$$m = \frac{DT_0 T_g}{(T_g - T_0)^2 \ln 10}. \quad (4)$$

The m of the $\text{Ce}_{60}\text{Ni}_{10}\text{Al}_{10}\text{Cu}_{20}$ BMG evaluated at a heating rate of 20 K/min from Eq. (4) is 21. According to Angell's classification,^{7,8} strong liquids with an approximately Arrhenius temperature dependence of relaxation times have values of fragility lower than 30 with an estimated lower limit of about 16 (e.g., for oxide glass of SiO_2 , GeO_2 , etc). Fragile liquids such as polymers and ionic melts display values of fragility above 100. The small value of m for the Ce-based alloy is very close to the strong limit and smaller than that of Zr- ($m=34-39$),³⁵ La- ($m \approx 32$),³⁵ Fe- (m

$=34-37$),³⁶ Mg- ($m=41$),³⁵ Pr- ($m=31$),⁴ and Pd-based ($m \approx 41$)³⁵ BMG's (all these m values are evaluated at 20 K/min). The small value of m demonstrates that the Ce-based liquid belongs to the strong family being less sensitive to the temperature changes and more stable than fragile liquids.^{7,8} The strong liquid behavior in the Ce-based alloy must have structural origin. Busch *et al.*³⁷ have proposed several reasons to explain why the ZrTiCuNiBe BMG-forming alloys are stronger supercooled liquids. The structural studies of these strong liquids indicate that they possess a relatively small amount of free volume and significant chemical short-range ordering in the melt.³⁷ Therefore, the strong liquid behavior of the Ce-based alloys should come from the much random packed liquid structure having less free volume. Even though there is no direct connection between the value of m and the GFA of an alloy,³⁸ the small value of m and larger value of T_{RG} and γ (see Table I) confirm that the Ce-based BMG can be classified into one of the excellent metallic glass formers, whose metastable equilibrium supercooled liquid is fairly stable.

D. Remarkable phonons softening behavior

Table III contrasts the values of ρ , v_l , and v_s as well as the elastic constants and θ_D for the $\text{Ce}_{70}\text{Al}_{10}\text{Ni}_{10}\text{Cu}_{10}$ BMG, typical $\text{Zr}_{41}\text{Ti}_{14}\text{Cu}_{12.5}\text{Ni}_{10}\text{Be}_{22.5}$ BMG (vit1) and their corresponding crystallized state. For comparison, the acoustic and elastic constants of the typical Cu-based BMG and Mg-based BMG as well as their fully crystallized states are listed in Table III.³⁹ The large changes in v_s (21%), v_l (13%),

TABLE III. The elastic constants of the $\text{Ce}_{70}\text{Al}_{10}\text{Ni}_{10}\text{Cu}_{10}$ and $\text{Zr}_{41}\text{Ti}_{14}\text{Cu}_{12.5}\text{Ni}_{10}\text{Be}_{22.5}$ alloys in their glassy and fully crystallized states. The Cu- and Mg-based BMG's with markedly different glass transition temperatures are also listed for comparison. Y_a and Y_c stand for the elastic constants and θ_D of these alloys in glassy and crystallized states, respectively. The elastic constants of the component elements in the $\text{Ce}_{70}\text{Al}_{10}\text{Ni}_{10}\text{Cu}_{10}$ alloy from references, and the calculated elastic constants of the $\text{Ce}_{70}\text{Al}_{10}\text{Ni}_{10}\text{Cu}_{10}$ alloy based on the elastic constants of its components are also listed.

Composition		ρ (g/cm ³)	V_l (km/s)	V_s (km/s)	E (GPa)	G (GPa)	K (GPa)	θ_D (K)	$\langle \mu^2 \rangle$ (Å ²)
$\text{Ce}_{70}\text{Al}_{10}\text{Ni}_{10}\text{Cu}_{10}$ ($T_g=359$ K)	glassy	6.670	2.521	1.315	30.3	11.5	27.0	144	1.18
	crystallized	6.711	2.884	1.590	43.5	17.0	33.2	174	0.81
	$(Y_c - Y_a)/Y_a$ (%)	0.6	14.4	20.9	43.6	47.8	22.9	20.8	-31.4
	Calculated								
$\text{Ce}_{70}\text{Al}_{10}\text{Ni}_{10}\text{Cu}_{10}$					42.9	17.5	29.1		
Ce (Ref. 46)					34	14	22		
Al (Ref. 46)					70	26	77		
Ni (Ref. 46)					200	83	180		
Cu (Ref. 46)					130	47	140		
$\text{Zr}_{41}\text{Ti}_{14}\text{Cu}_{12.5}\text{Ni}_{10}\text{Be}_{22.5}$ (Ref. 40) ($T_g=623$ K)	glassy	6.125	5.174	2.472	101.2	37.4	114.1	327	0.64
	crystallized	6.192	5.446	2.807	128.7	48.8	118.6	371	0.58
	$(Y_c - Y_a)/Y_a$ (%)	1.1	5.2	13.5	27.2	30.3	3.9	13.4	-9.4
	Calculated								
$\text{Ce}_{70}\text{Al}_{10}\text{Ni}_{10}\text{Cu}_{10}$									
glassy		8.315	4.62	2.108	101.1	36.9	128.2	282	
crystallized		8.363	4.797	2.342	123.3	45.9	131.3	312	
$(Y_c - Y_a)/Y_a$ (%)		0.58	3.8	11.1	22.0	24.4	2.4	10.6	
$\text{Cu}_{60}\text{Zr}_{20}\text{Hf}_{10}\text{Ti}_{10}$ (Ref. 39) ($T_g=754$ K)	glassy	3.98	4.22	2.22	51.3	19.6	44.7	272.9	
	crystallized	4.00	4.53	2.45	62.0	24.0	50.2	300.9	
	$(Y_c - Y_a)/Y_a$ (%)	0.5	7.3	10.3	19.9	22.4	12.3	10.2	
	Calculated								
$\text{Mg}_{65}\text{Cu}_{25}\text{Tb}_{10}$ (Ref. 39) ($T_g=414$ K)									
glassy		3.98	4.22	2.22	51.3	19.6	44.7	272.9	
crystallized		4.00	4.53	2.45	62.0	24.0	50.2	300.9	
$(Y_c - Y_a)/Y_a$ (%)		0.5	7.3	10.3	19.9	22.4	12.3	10.2	

$E(43.5\%)$, $G(47\%)$, $K(22.9\%)$, and $\theta_D(20.6\%)$ and small change in $\rho(0.6\%)$ between the glassy and crystallized states for the Ce-based BMG can be seen in Table III. The remarkably large changes of elastic moduli in the BMG relative to its crystallized state mean that markedly softening of long-wavelength transverse as well as longitudinal acoustic phonons in the BMG. However, only the markedly softening of the transverse elastic modulus (normally $\sim 20\text{--}35\%$ change in G) can be observed in amorphization process²⁹, and various other BMG's.^{39–41} Table III contrasts the relative changes of ρ , v_s , G , K , and θ_D of the $\text{Ce}_{70}\text{Al}_{10}\text{Ni}_{10}\text{Cu}_{10}$ BMG and vit1 compared with their crystallized states. For vit1, large changes in $v_s(13.5\%)$, $\theta_D(13.4\%)$, and $G(30.3\%)$ but much smaller changes in $v_l(5.2\%)$ and $K(3.9\%)$ between the two states. However, the Ce-based BMG shows substantially larger softening in G , E , and θ_D and large softening in K and longitudinal acoustic velocity as well. This phenomenon is different from that of other BMG's.^{17,29} This unusual softening concerning the elastic phonons of the Ce-based BMG may result from the intrinsic structural feature of the Cerium base, and it could be due to the low glass transition temperature of the alloy as well. However, Table III shows that the vit1 ($T_g=623$ K), the $\text{Cu}_{60}\text{Zr}_{20}\text{Hf}_{10}\text{Ti}_{10}$ BMG with higher T_g ($T_g=754$ K),³⁹ and the $\text{Mg}_{65}\text{Cu}_{25}\text{Tb}_{10}$ BMG with low T_g ($T_g=414$ K),³⁹ which have markedly different glass transition temperatures, exhibit the similar softening behavior. The comparison indicates that the unusual softening in the Ce-based BMG's mainly result from the intrinsic structural feature of the Cerium base that is of variable electronic structure and dual valency states, and only small amount of energy is required to change the relative occupancy of the electronic levels.⁶ The small density change suggests that the Ce-based BMG contains less density of free volume and has more random packed microstructure compared with vit1. This result is in good accordance with the strong liquid behavior concerning the temperature dependence of viscosity of Ce-based BMG's.³⁷

In order to further understand the phonons softening behavior, the correlation between the elastic constants of the glassy state and its pure metallic components is considered. It has been shown that the compression of the $\text{Pd}_{40}\text{Ni}_{20}\text{P}_{20}$ metallic glass is similar to those of crystalline nickel and palladium,⁴² and that the compression curves of Zr-based and Pd-based BMG's have a correlation with those of their metallic components and represent a rough average of those for these elements, indicating that the short-range order structure of these BMGs has a close correlation with the atomic configurations of their metallic components.^{43,44} For an alloy, its elastic constants may agree well with the calculated value expressed by the relation^{45,46}

$$M^{-1} = \sum f_i M_i^{-1}, \quad (5)$$

where M denotes any elastic constants and f_i is the atomic percentage of the constituent element. The elastic constants of the Ce, Ni, Al, and Cu components,⁴⁷ the calculated elastic constants of the $\text{Ce}_{70}\text{Al}_{10}\text{Ni}_{10}\text{Cu}_{10}$ alloy according to Eq. (5), and experimental results of the $\text{Ce}_{70}\text{Al}_{10}\text{Ni}_{10}\text{Cu}_{10}$ alloy in glass and crystallized states are also shown in Table III. The

calculated elastic constants of the Ce-based alloy are very close to those of its crystalline state. Except for K , a large difference between calculated and experimental values of E , G , and σ of the BMG exists, indicating that the elastic constants of the BMG should not be simply described by a rough average of those of component elements. Therefore, the above results further confirm that the large softening of the Ce-based BMG is attributed to its intrinsic glassy structure.

The large elastic phonons softening behavior of the Ce-based BMG should also have close relation with its strong liquid behavior concerning the temperature dependence of viscosity. Lam *et al.*²⁹ point that the softening of G associates with critical static atomic displacement $\langle \mu \rangle$ and anharmonic vibration in a metallic glass. The softening of the transverse elastic modulus of metallic glasses was also anticipated theoretically.⁴⁸ Table III shows that the phonons softening behavior of the Ce-based BMG can also be demonstrated by its large $\langle \mu^2 \rangle$, which is related to T_m and θ_D as⁴⁹ $\langle \mu^2 \rangle = 9h^2 T_m / (M k_B \theta_D^2)$. The $\langle \mu^2 \rangle$ is a general measure of the chemical and topological disorder and hence can be used as a general disorder parameter for characterizing a glassy solid.⁴⁹ Miglio⁵⁰ also found that the larger $\langle \mu^2 \rangle$ gave rise to a lower elastic energy. As shown in Table III, the increase of $\langle \mu^2 \rangle$ in the BMG relative to its crystallized state is larger than that of vit1, confirming the more disordered structure of the BMG having very low elastic energy and showing softening behavior.

IV. CONCLUSIONS

The CeAlNiCu BMG system has been obtained by a conventional Cu-mold cast method. The BMGs exhibit a wide supercooled region up to 78 K, very low glass transition temperature ($T_g=359$ K) and Debye temperature ($\theta_D=144$ K). Ultrasonic measurements demonstrate that the Ce-based BMG's are the softest in elastic moduli, and the softer behavior in elastic constants compared to other BMG's maybe due to the low glass transition temperature of the Ce-based alloy.

The fragility parameter of the typical $\text{Ce}_{60}\text{Al}_{10}\text{Ni}_{10}\text{Cu}_{20}$ BMG obtained from the heating rate dependence of the glass transition is 21, indicating the strong liquid behavior according to Angell's classification of glass forming liquids. A large softening of acoustic phonons in the BMG relative to its crystalline state is observed, which demonstrates that the unusual phonon softening of the Ce-based BMG originates from its intrinsic microstructural features and the strong liquid behavior concerning the temperature dependence of viscosity.

ACKNOWLEDGMENTS

Financial support from the National Science Foundation of China (Grants Nos. 50321101 and 50371097), Science and Technology Department of Beijing City (Grant No. H02040030320), and Chinesisch-Deutsches Zentrum Für Wissenschaftsfoerderung (Grant No. GZ032/7) is acknowledged. Experimental assistance from Z.F. Zhao is appreciated.

*Email address: whw@aphy.iphy.ac.cn

- ¹W. L. Johnson, MRS Bull. **24**, 42 (1999); W. H. Wang, C. Dong, and C. H. Shek, Mater. Sci. Eng., R. **44**, 45 (2004).
- ²A. Inoue, Acta Mater. **48**, 279 (2000).
- ³Z. Zhang, R. J. Wang, B. C. Wei, and W. H. Wang, Appl. Phys. Lett. **81**, 4371 (2002).
- ⁴Z. F. Zhao, D. Q. Zhao, and W. H. Wang, Appl. Phys. Lett. **82**, 4699 (2003).
- ⁵F. Guo, and S. J. Poon, Appl. Phys. Lett. **83**, 2575 (2003).
- ⁶Z. Q. Zheng, *Rare Earth Functional Materials* (Chemical Industry Press, China, 2003), pp. 433–460.
- ⁷C. A. Angell, J. Non-Cryst. Solids **73**, 1 (1985).
- ⁸C. A. Angell, Science **267**, 1924 (1995).
- ⁹W. H. Wang, R. J. Wang, and M. X. Pan, Appl. Phys. Lett. **74**, 1803 (1999); D. Schreiber, *Elastic Constants and Their Measurement* (McGraw-Hill, New York, 1973).
- ¹⁰D. Turnbull, Contemp. Phys. **10**, 473 (1969).
- ¹¹Z. P. Lu and C. T. Liu, Phys. Rev. Lett. **91**, 115505 (2003).
- ¹²Z. P. Lu, T. T. Goh, Y. Li, and S. C. Ng., Acta Mater. **47**, 2215 (1999).
- ¹³T. Waniuk, J. Schroers, and W. L. Johnson, Phys. Rev. B **67**, 184203 (2003).
- ¹⁴N. Nishiyama, M. Horino, and A. Inoue, Appl. Phys. Lett. **76**, 3914 (2000).
- ¹⁵O. N. Senkov and D. B. Miracle, MRS Bull. **36**, 2183 (2001).
- ¹⁶F. R. de Boer, R. Boom, W. C. M. Matterns, A. R. Miedema, and A. K. Niessen, *Cohesion in Metals* (North-Holland, Amsterdam, 1988).
- ¹⁷W. H. Wang, L. L. Li, M. X. Pan, and R. J. Wang, Phys. Rev. B **63**, 052204 (2001); W. H. Wang, P. Wen, and R. J. Wang, J. Mater. Res. **18**, 2747 (2003).
- ¹⁸B. Hartmann and J. Jarzynski, J. Acoust. Soc. Am. **74**, 1346 (1974).
- ¹⁹H. E. Kissinger, J. Res. Natl. Bur. Stand. **57**, 217 (1956).
- ²⁰R. A. Ligerio, J. Vázquez, P. Villares, and R. Jiménez-garay, Mater. Lett. **8**, 6 (1989).
- ²¹Z. X. Wang, D. Q. Zhao, M. X. Pan, W. H. Wang, Okada, and W. Utsumi, J. Phys.: Condens. Matter **15**, 5923 (2003).
- ²²N. Mitrovic, S. Roth and J. Eckert, Appl. Phys. Lett. **78**, 2145 (2001).
- ²³J. M. Borrego A. Conde, S. Roth, and J. Eckert J. Appl. Phys. **92**, 2073 (2002); J. M. Borrego, C. F. Conde, A. Conde, S. Roth, H. Grah, A. Ostwald, and J. Eckert, J. Appl. Phys. **92**, 6607 (2002).
- ²⁴Y. X. Zhuang, W. H. Wang, and D. Q. Zhao, Appl. Phys. Lett. **75**, 2392 (1999).
- ²⁵N. Nishiyama and A. Inoue, Acta Mater. **47**, 1487 (1999).
- ²⁶A. Inoue, *Bulk Amorphous Alloys, Practical Characteristics and Applications, Materials Science Foundation* (Trans. Tech, Switzerland), p. 6.
- ²⁷Z. Li, H. Y. Bai, M. X. Pan, and W. H. Wang, J. Mater. Res. **18**, 2208 (2003).
- ²⁸T. M. Lasocka, Mater. Sci. Eng. **23**, 173 (1976).
- ²⁹P. R. Okamoto, N. Q. Lam and L. E. Rehn, *Solid State Physics*, edited by H. Ehrenrein, and F. Spapen (Academic, San Diego, 1999), Vol. 52, pp. 1–135.
- ³⁰R. Busch and W. L. Johnson, Appl. Phys. Lett. **72**, 2695 (1998); R. Busch, Y. J. Kim, and W. L. Johnson, J. Appl. Phys. **77**, 4039 (1995).
- ³¹W. H. Wang, Y. X. Zhuang, M. X. Pan, and Y. S. Yao, J. Appl. Phys. **88**, 3914 (2000).
- ³²R. Brüning and K. Samwer, Phys. Rev. B **46**, 11 318 (1992).
- ³³R. Böhmer and C. A. Angell, Phys. Rev. B **45**, 10 091 (1992).
- ³⁴R. Böhmer, K. L. Ngai, C. A. Angell, and D. J. Plazek, J. Chem. Phys. **99**, 4201 (1993).
- ³⁵D. N. Perera, J. Phys.: Condens. Matter **11**, 3807 (1999).
- ³⁶J. M. Borrego, A. Conde, S. Roth, and J. Eckert, J. Appl. Phys. **92**, 2073 (2002).
- ³⁷R. Busch, E. Bakke and W. L. Johnson, Acta Mater. **46**, 4725 (1998); H. Tanaka, Phys. Rev. Lett. **90**, 055701 (2003).
- ³⁸J. M. Borrego, C. F. Conde, A. Conde, S. Roth, H. Grah, A. Ostwald, and J. Eckert, J. Appl. Phys. **92**, 6607 (2002).
- ³⁹W. H. Wang, B. Zhang, and R. J. Wang (unpublished); X. K. Xi, W. H. Wang, J. Non-Cryst. Solids (to be published).
- ⁴⁰W. H. Wang, H. Y. Bai, R. J. Wang, and D. Jin, Phys. Rev. B **62**, 25 (2000).
- ⁴¹L. E. Rehn and P. R. Okamoto, Phys. Rev. Lett. **59**, 2987 (1987).
- ⁴²E. F. Lambson, Phys. Rev. B **33**, 2380 (1986).
- ⁴³L. M. Wang and W. H. Wang, Appl. Phys. Lett. **77**, 3734 (2000).
- ⁴⁴W. H. Wang, M. X. Pan, and D. Q. Zhao, Appl. Phys. Lett. **79**, 3947 (2001).
- ⁴⁵Z. Zhang, R. J. Wang, M. X. Pan, and W. H. Wang, J. Phys.: Condens. Matter **15**, 4503 (2003).
- ⁴⁶A. Voronel and S. J. Rabinovich, J. Phys. F: Met. Phys. **17**, L193 (1987).
- ⁴⁷[http:// www.webelements.com](http://www.webelements.com)
- ⁴⁸D. Weaier, Acta Metall. **19**, 779 (1971).
- ⁴⁹N. Q. Lam, L. E. Rehn, and P. R. Okamoto, MRS Bull. **19**, 41 (1994).
- ⁵⁰L. Miglio, Appl. Phys. Lett. **74**, 3654 (1999).